Evaluation of 3D Mapping Experimental Non-Intrusive Methods for Multiphase Flows

Christopher Poette and Philippe Reynier
Ingénierie et Systèmes Avancés, Pessac, France
Email: Philippe.Reynier@isa-space.eu

ABSTRACT

The present contribution focuses on the evaluation of non-intrusive 3D mapping experimental methods for the investigation of multiphase flows during tank sloshing. This problem is a key issue for launchers and satellites since the feeding in propellants has to be ensured during flight and manoeuvres. At first, an extensive survey of non-intrusive experimental techniques of interest for multiphase flows has been carried out. This task has accounted for new innovative methods developed for space and non-space applications with a focus on the methods used in medicine and other fields such as ultrasound techniques. A particular care has been given to electrical and ultrasonic tomography techniques since they are both non-intrusive, non-invasive, low cost, fast and simple to operate, and suitable for real time measurements.

Electrical tomography techniques have demonstrated convincing capabilities for multiphase flow visualization and present numerous advantages for industrial processes and multiphase flow measurements. Ultrasound experimental techniques are extensively used in medicine for a wide range of investigations. They are also largely used for material analysis and fluid mechanics. As a consequence since several years, ultrasound tomography has been applied to multiphase flows. Application of the method to annular, sludge, slug and bubbly flows has demonstrated the potential of this technique for multiphase flow investigations. Additionally, in the context of launchers this technique presents an advantage in term of safety.

Using the available results, the advantages and disadvantages of ultrasonic and electrical methods have been identified and this leads to the conclusion that the ultrasonic tomography possesses the best potential for the final application. Finally, using the available experimental results obtained using ultrasound tomography for the mapping of multiphase flows, numerical simulations have been performed to proceed to their reconstruction. This provides a cross-check between the experimental data and the numerical predictions in order to assess the suitability of the techniques for future studies.

1. INTRODUCTION

The experimental investigation of propellant tank sloshing is a key issue [1] for the development of future launchers, the capability of ensuring the alimentation of rocket engines in case of engine re-ignition in microgravity is, indeed, a crucial condition for providing the launcher the capability of delivering several spacecraft on different trajectories. The main concern, when investigating tank sloshing, is the lack of experimental data due to the difficulty of carrying out measurements in a tank for cryogenic conditions in microgravity. Several approaches are currently available for performing tests in microgravity environment: Drop tower, parabolic flights, sounding rockets, or experiments on-board the International Space Station (ISS). The different means with the level of microgravity and the test duration are resumed in Figure 1.

Beyond the microgravity aspects, there are some difficulties to collect experimental data for in-flight configurations. Usually, tests are done with gyroscopes and accelerometers [2] but this provides a limited amount of information. Information like the position of the liquid interface is not available since there is no possibility to measure it, with the usual experimental techniques and without perturbing the flow. Another possibility is to visualize the flow with a video camera [3] but this does not provide quantitative data on void fraction, pressure, velocity, and interface location.

In order to investigate the ways to fill this technical gap, an assessment of recent experimental methods is performed in this review. For avoiding the problem of flow perturbation the activity has been restricted to non-intrusive techniques. The work has been largely focused on the methods used in medicine like the ultrasound techniques, but other approaches based on ultrasound or electrical methods used in other domains such as the oil and gas industry and the chemical engineering have been also considered. Some reviews [4-6] considering different innovative techniques have been already carried out and have been largely used for supporting this assessment.

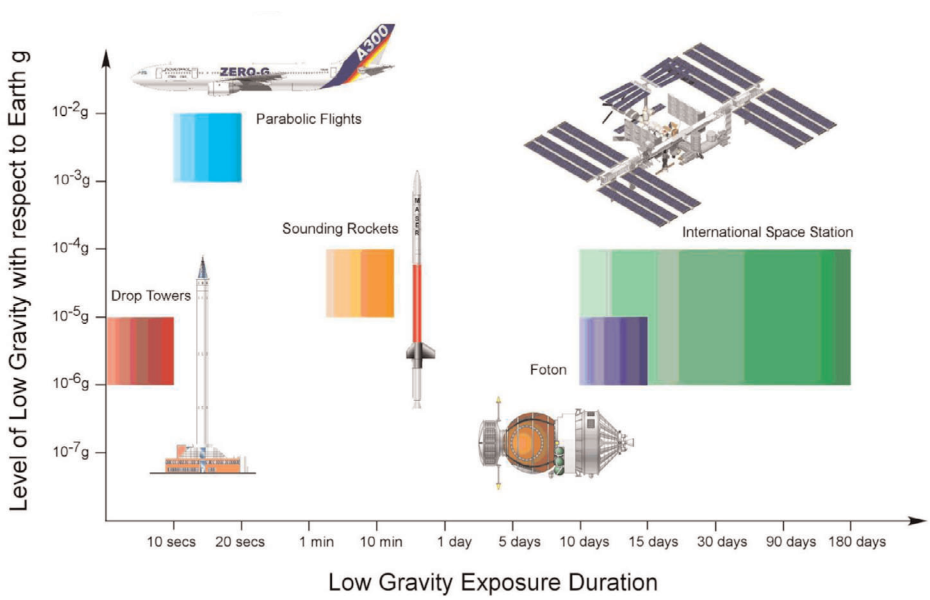

Figure 1: Microgravity platforms (credit ESA/ESTEC)

Among the measurement techniques, recently developed, the non-intrusive techniques as defined in Figure 2, are the most attractive. The different approaches of interest for the current activity are briefly described hereafter:

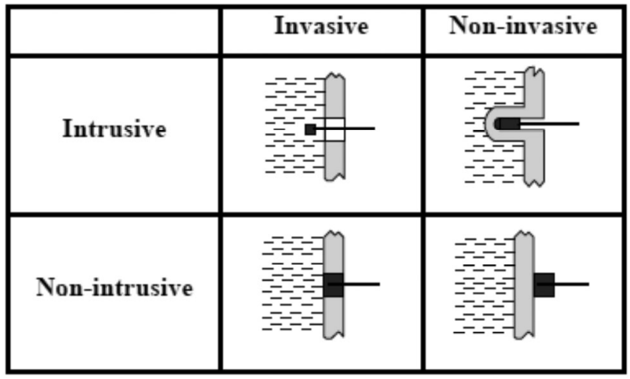

Figure 2: Non-invasive and non-intrusive methods [5]

- X, γ and β ray attenuation measurements: When a beam of radiation cross a two-phase mixture, it is attenuated and the degree of attenuation can be linked to the flow composition.
- Electric methods: Electrical impedance method is based on the fact that the fluid flowing in the measurement section is similar to an electrical conductor. In oil mixtures, the electrical impedance is large and can be difficult to measure reliably. For water flows, a short-circuiting effect can occur. According to [4], impedance methods suffer from two major limitations: they cannot be used over the full component fraction range and are flow-regime dependent. Other electrical methods are based on electrical capacitance and electrical charge tomography:
- Nuclear magnetic resonance (NMR) method: This method involves measurements of NMR signal from ^{1}H nuclei in the liquid that can be related to the two-phase mixture density. One of the main drawbacks [4] is that it requires a non-metallic pipe section close to the measurement point to allow penetration of the radio frequency field.
- Microwave technology: This technique is based on the interaction between microwaves and the media of propagation (liquid or gas) that is determined by the relative permittivity. Operation principles of this technology have been reviewed by Nyfors [7].
- Ultrasound probes: Although this technique is not invasive and allows quick multiphase flow measurements, their accuracy might deteriorate for high gas fraction. Acoustic emissions has been largely used in hydraulics: turbulence noise from vortices, cavitation, bubble formation growth and collapse, mixture interaction, flows in piping, bursting, flashing and water hammer, liquid drops impacting a free surface, leakage, oceanic noise…
- γ-neutron reaction method: Neutrons are emitted when g-rays pass through heavy water. Since emission depends on heavy water, this technique has limited applications (the liquid phase has to contain heavy water).

Most of these techniques, like X-ray tomography and ultrasound techniques are widely used in medicine. However, for other applications, radiation methods due to the presence of ionizing radiation are dangerous. But even with this restriction, X-ray tomography has already been applied to investigate flow structures in fluidized beds as reported in [5] where this system has measured solid concentration up to 20%. NMR has been used to investigate solid-fluid suspensions.

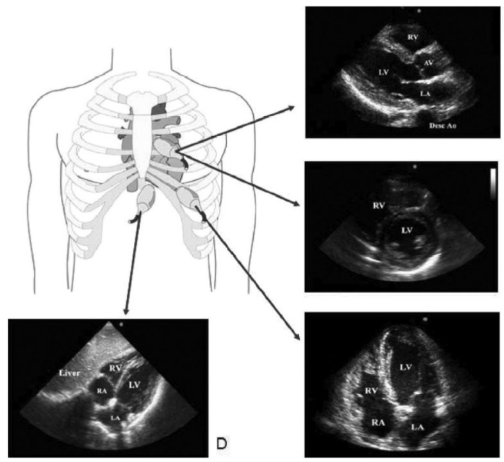

Figure 3: Windows for hart exploration using ultrasound probes (from [8])

It seems that ultrasonic tomography is the most popular. It has been successfully applied in flow measurements and is extensively used in medicine [8-12] as highlighted in Figure 3. However, with this method, it is difficult to collimate and problems occur due to reflections within enclosed spaces, such as metal pipes. The application of ultrasonic tomography encounters some limitations: waves can be attenuated; in two-phase flows the presence of interfaces limits the resolution; at a gas-liquid interface, the reflection rate is almost 90%. As a consequence, this technique is more adapted to bubbly or particulate flows and for some authors, holdups of 20% are a reliable limit for its application. Nevertheless, very promising results have been recently obtained for high gas fractions (up to 50%) [4-5].

The study has been split in two main tasks. At first, the different issues related to the experimental investigation of cryogenic fluids have been identified and an assessment of innovative non-intrusive techniques carried out. A particular care has been given to the results obtained for multiphase flows using ultrasound and electrical tomographic techniques to estimate the potential of these methods for the experimental investigation of tank propellant sloshing. This assessment has highlighted the potential of ultrasound tomography for this objective. In a second step, experimental data obtained with ultrasound tomography have numerically reconstructed to estimate the suitability of this technique for 3D mapping of multiphase flows. These numerical simulations have been performed using OpenFoam a computational fluid dynamics solver. Multiphase flows have been simulated for a wide range of conditions (stratified, annular, bubbly and slug) for assessing the potential of the ultrasonic tomography for sloshing encountered in space applications.

2. ASSESSMENT OF NON-INTRUSIVE TECHNIQUES

In the frame of this activity a extensive literature review on non-intrusive experimental methods has been undertaken. This review has been more focused on the results obtained using electrical and ultrasonic tomographic methods. The potential issues for investigating cryogenic fluids have been also identified. The different points are detailed hereafter where the most remarkable elements on the experimental methods have been synthetized.

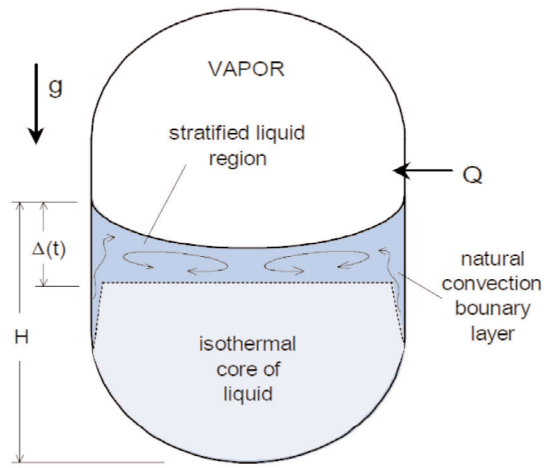

Figure 4: Cryogenic liquid stratification [13]

2.1 ISSUES RELATED TO CRYOGENIC FLUIDS

Cryogenic fluids are low-permittivity fluids so the capacitance variations between the fluid and the gas are rather small and lead the experimental methods to reach their measurement limitations. Some setups have the particularity to increase the sensitivity to dielectric permittivity variations and preserve the ability to detect small perturbations by using a spatial filtering approach that allows an improvement of the signal-to-noise ratio.

Conductance probes have been already applied to velocity measurements of liquid hydrogen flows [13] in conveyor pipes. They have also been used to design flowmeters for slush hydrogen flows [14]. In the frame of this review no results on cryogenic flows based on ET (Electrical Tomography) applications were found.

Other problems occur with cryogenic fluids. The vapour pressure of such fluids is not greatly different from the tank pressure, which can easily lead to local boiling of vaporization of the fluid and pressure rise in the tank. In addition, the liquid temperature is generally far from being uniform [1,13] especially at the interface due to natural convection (even in low gravity where buoyancy forces can be significant for large tanks). The isothermal area and natural convection for a cryogenic tank are represented in Figure 4. The difference of temperature between the fluid and the external domain is also important and the tanks need to be efficiently insulated to avoid the accentuation of such phenomenon. Changes of state and temperature modify electrical properties of the domain and then the measured values.

2.2 ASSESSMENT OF ELECTRICAL TOMOGRAPHIC TECHNIQUES

Electrical measurement techniques present numerous advantages for industrial processes and multiphase flow measurements as being non-intrusive, non-invasive, low cost, fast and simple to operate, and suitable for real time measurements [15-17]. Electrical Capacitance Tomography (ECT) has been widely investigated in literature [15-16] with the elaboration of robust image reconstruction algorithms and the possibility of 3D mapping with Electrical Capacitance Volume Tomography (ECVT). Nevertheless, the ill posedness of the equations and sensor limitations restrict the use of electrical tomography techniques due to a low spatial resolution [15-16,18-19]. The main disadvantage of electrical methods is the fact that electrical properties such as conductivity and permittivity are temperature dependent. This is particularly the case for conductivity has pointed out by Elkow [20]. As a consequence, their application to multiphase cryogenic flows will require additional efforts to assess their applicability at low temperatures with potential phase changes due to thermal effects. Another point to be considered is the use of electrical fields in propergols tanks; this could raise some issues related to safety for the launcher itself.

Actually, the most promising ET method is the multimodal tomography but its maturity is not yet reached and this objective will require additional efforts related to sensor development and image reconstruction algorithms in order to improve the technique. Multimodal tomography is an imaging system exploiting multiple electrical properties. An example is given in Figure 5 that shows the images of two spheres obtained by electrical tomography using permittivity and conductivity distributions.

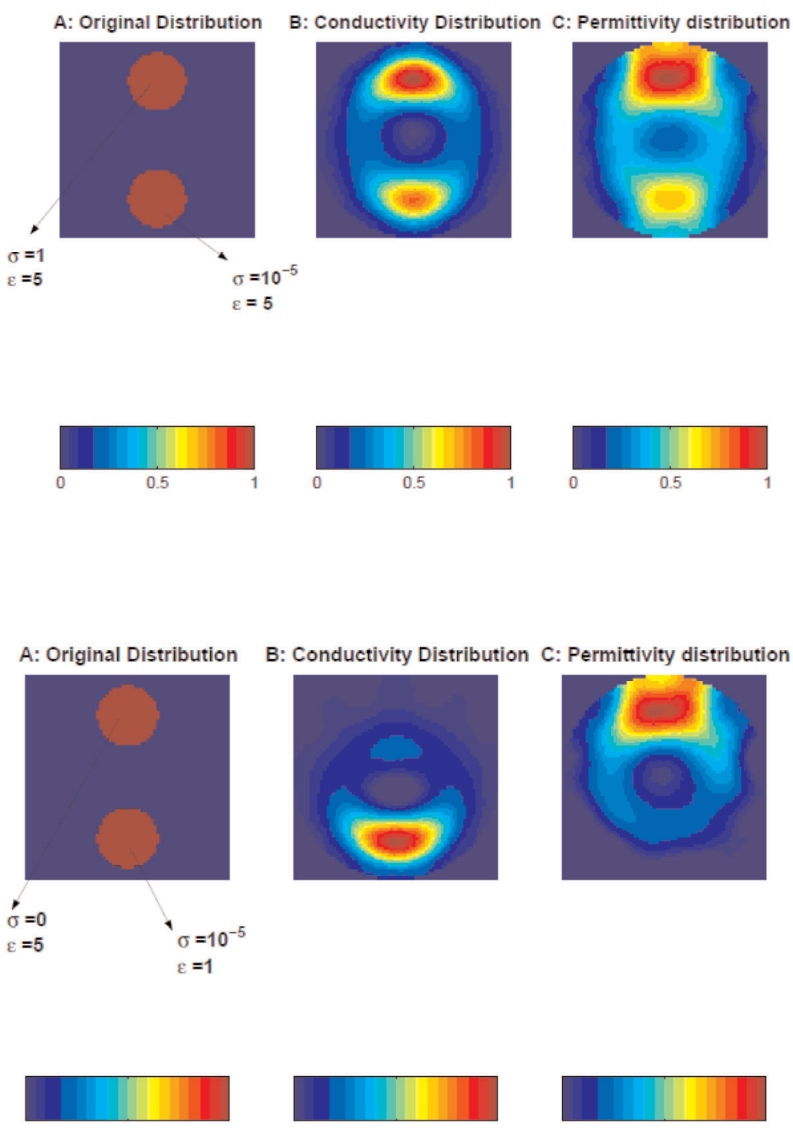

Figure 5: Image reconstruction with multimodal tomography for a two-sphere case with different conductivity (s) and permittivity (e). The original distribution is depicted on the left [16]

2.3 SYNTHESIS ON ULTRASONIC TOMOGRAPHY

Ultrasound is able to detect changes in acoustic impedance, which is closely related to the media density and then complements other imaging techniques such as electrical capacitance tomography and electrical impedance tomography [21]. Ultrasonic techniques can be used to image gas component in air/water mixtures due to the large density differences (while capacitance techniques can be used to image water component) [22]. This has built the success of acoustic Doppler ultrasound techniques for medical investigations.

Since the first medical application of ultrasound technique carried out in 1942 by Dussik for observing deviations in median intracranial structures, ultrasound experimental techniques have been widely used for non-intrusive measurements. Ultrasonic sensors have a long history of success and have been largely utilized in fields like medicine, biology [23], material analysis [24], and metallurgy [25], and fluid mechanics [4] to investigate experimentally turbulence noise from vortices, cavitation, bubble formation growth and collapse, mixture interaction, flows in piping, bursting, flashing and water hammer, liquid drops impacting a free surface, leakage, and oceanic noise. An example of result obtained in biology is shown in Figure 6.

The recent development of ultrasonic tomography for multiphase flow applications is very promising. This new technique is able to provide mapping of bubbly, slug and annular flows in pipes for large gas fractions [5]. The advantage of ultrasonic tomography is its only dependence on acoustic impedance, which depends mostly on the medium density.

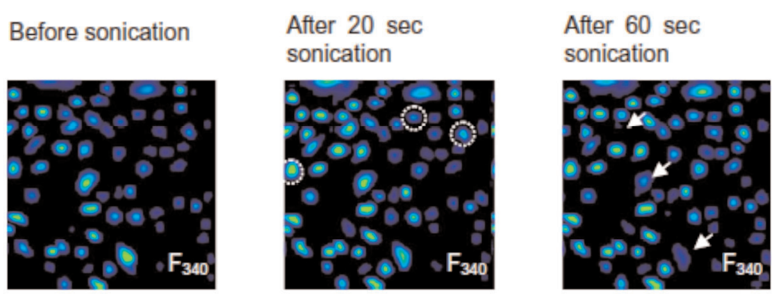

Figure 6: Increase of fluorescence by Ca2+ during ultrasound irradiation of a plasma membrane [23]

2.4 ASSESSMENT OF OTHER INNOVATIVE TECHNIQUES

Some other non-intrusive methods assessed in this strong possess strong capabilities for investigating multiphase flows. However, due to some of their characteristics or cost some of them can be hardly selected for investigating sloshing during in-flight experiments.

Holographic interferometry is very attractive for studying gas phase flows or flows with a dispersed phase (particles, sprays) [26-28]. However, during this review an application of this technique to a multiphase flow with two continuous phases separated by an interface was not identified. For using this technique two lasers are needed, this has some impacts as far as the cost and room taken by the experimental set-up are considered. This technique can be envisaged with some difficulty for studying the sloshing of liquids with a strong constraint in terms of space, as encountered for a flight experiment.

Nuclear magnetic resonance presents some issues since the media to be investigated shall contain ^{1}H nuclei, and a non-metallic section has to be available to allow the penetration of the radio frequency field within the flow [29]. Other electromagnetic methods [30] based on the use of electromagnetic sensors could be difficult to select for an in-flight experiment due to the sensitivity of on-board electronics to magnetic fields.

If we consider radiation techniques they are expensive and so far no demonstration of their capabilities for 3D mapping has been found. β-ray techniques will be difficult to use on large vessels since the β -rays are absorbed more readily than g-rays. For other radiation methods (X and γ-rays) the attenuation will have to be assessed carefully. However, γ-ray methods have been already applied to multiphase flows [31-32-33] and γ-ray tomography could be used for investigating sloshing even if the associated cost could be high. Additionally, this technique requires the presence of a radioactive source (^{137}Cs) on-board and this could present other issues related to safety.

Among the methods screened in this technical note microwave based experimental techniques could be very attractive [34-35-36] but they suffer from a major drawback due to the necessity to have some water in the liquid phase.

2.5 SYNTHESIS

Tomographic techniques based on ultrasound or electrical approaches are being available for 3D mapping of multiphase flows. If progresses are still needed for improving the image reconstruction algorithms as well as the sensor capabilities, valuable results have been already produced. Both techniques can be used to perform non-intrusive measurements within metallic vessels.

Among the electrical tomographic methods, capacitance tomography is the most popular and seems to have the best potential for future applications. The results obtained with ultrasound tomography highlight its capabilities not only at low holdups of gas or solid but also at high gas fractions since this methods is able to produce valuable results for slug flows in pipe.

If cryogenic flows have to be investigated, when comparing ultrasound and capacitance tomography's, the ultrasound approach might be more attractive since the ET methods are all based on electrical properties of the medium that can have strong variations under temperature (or phase change) effects. Ultrasound methods are based on the acoustic impedance, which is based on the medium density and sound speed. They are well adapted to locate a liquid/gas interface. A last point to be analysed will be the safety of the technique to perform measurements in propergols tanks. Here, ultrasonic tomography should have the advantage on an electrical technique.

3. NUMERICAL RECONSTRUCTIONS

For evaluating the capabilities of ultrasonic tomography, it is necessary to proceed to the reconstruction of some experimental measurements carried out using ultrasonic tomography. This will allow assessing the capabilities of the experimental technique by comparing the data with the numerical predictions of a CFD code. Among the results obtained using ultrasonic tomography, those published by Rahiman [5] are the most attractive. He has tested the method for a wide range of flow patterns: bubbly, annular, stratified, slug, and sludge flow conditions. However, these experiments have been mostly performed for static configurations, for this reason it has seemed opportune to complete the set of test cases with an experimental configuration, well documented, and that has been already numerically computed. For these different reasons, the study performed by Vallée et al [37] has been selected. In this study, a slug flow has been experimentally investigated and numerical reconstructed. The different experiments selected for the numerical simulations are detailed hereafter.

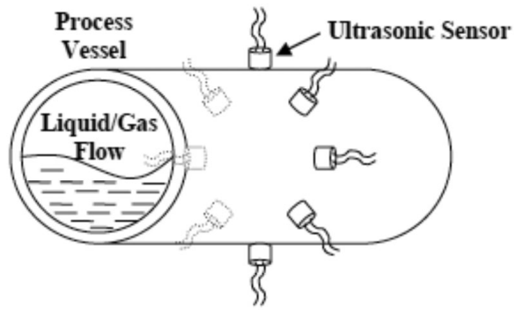

Figure 7: Sensor arrangement around a pipe [5]

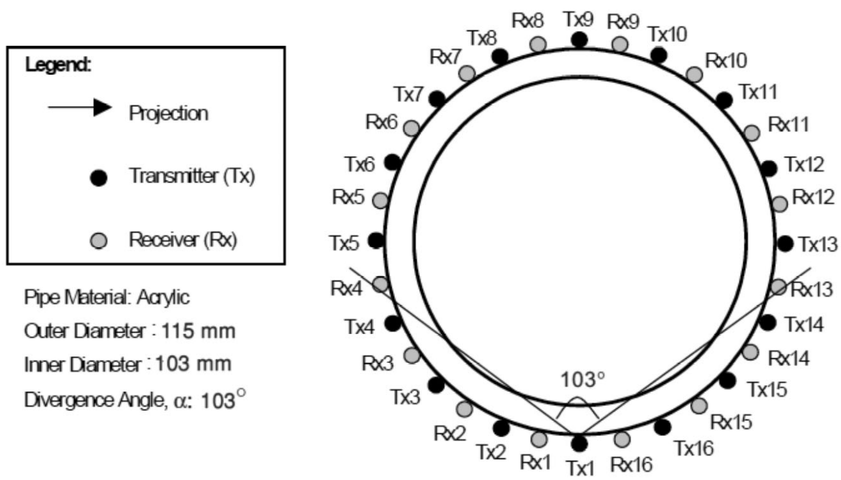

Figure 8: Experimental sensor configuration [5]

3.1 RESULTS OBTAINED BY ULTRASONIC TOMOGRAPHY

The flow configuration studied by Rahiman [5] is similar to the one shown in Figure 7. A circular pipe filled with water and air has been investigated using ultrasonic tomography for different flow conditions. The configuration was at room temperature 25°C and atmospheric pressure [38]. Tests were performed for a vertical configuration and static conditions for annular, stratified and bubbly flows. A test was also carried for an unsteady bubbly flow using a pump located at the bottom to inject bubbles.

The experimental sensor configuration with 16 pairs of ultrasonic sensors (receivers and transmitters) is shown in Figure 8. Sensors were mounted circularly on the surface of the test pipe as shown in this figure. The pipe section, on which the transducers were mounted, was in PVC. Since the use of ultrasonic methods in air is very inefficient due to the mismatch of the sensors impedance compared to air acoustic impedance, an acoustic coupling is needed between the sensor surface and the outer pipe wall; this is done using glycerine [39]. A wet coupling is used to allow easy application, good conduction of sound energy, and conformity to the void between the transducer and the surface. An acrylic pipe was chosen for the experiments. A steel pipe can be also used as demonstrated by Addali [4] on multiphase flows in pipes.

Using the experimental set-up shown in Figures 1 and 2 and a suitable image reconstruction algorithm, measurements within a liquid/gas flow have been performed. The inner and outer diameters of the pipe used for the experiments were 103 and 115 mm respectively. Pipe length was not documented.

The system has been shown capable of visualizing the internal characteristics of two-phase flows and provides the concentration maps of gas and liquid as shown in Figure 9. Three series experiments were carried out to investigate the flow: with 100% of water, ¼, ½, ¾ of water (bubbly and slug flows) and annular flows.

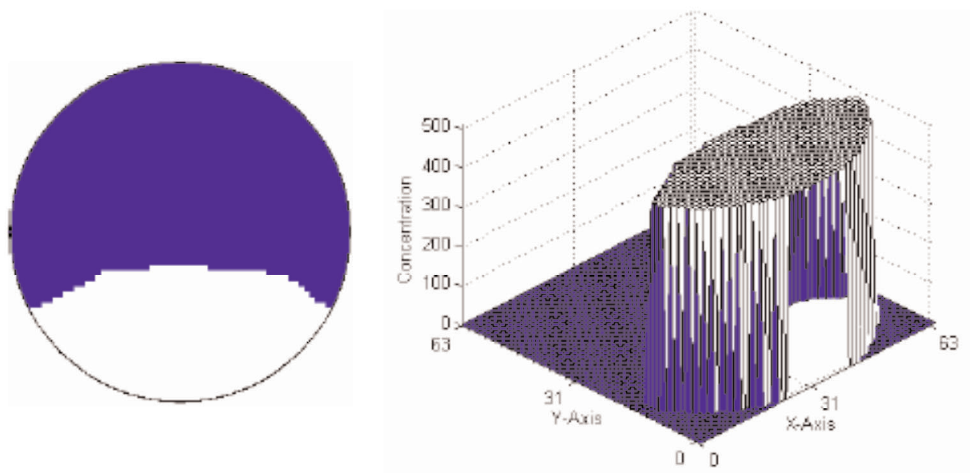

Figure 9: Reconstructed image of a sludge flow [5]

3.2 SLUG FLOW CONFIGURATION

Since the experimental results obtained by Rahiman [5], can only provide a qualitative comparison with the numerical simulations, it seems useful to have a more quantitative comparison between the numerical simulations and experimental data obtained for a complex multiphase flow with for objective to assess the numerical code capabilities. Among the available experimental results for multiphase flows, the experiments carried out by Vallée et al [37] presents several advantages. The experimental campaign has been carried out for slug flows in a rectangular channel. Additionally, the measurements have been numerically reconstructed using ANSYS-CFX by the authors. This will give also the opportunity to cross-check the comparisons between the different numerical simulations.

The air/water channel used by Vallée et al [37] for their experiments is shown in Figure 10. This rectangular channel is 8 m long and the length and width of the cross section are 100 and 30 mm respectively. The length to height ratio is 80. Water and air are injected separately at the inlet. Since inlet geometry produces flow perturbations, 4 wire mesh filters have been added to give a more homogeneous velocity profile at the inlet. Moreover, the filters induce a pressure drop that attenuates the effect of the pressure surge created by slug flows. Air and water flowrate are measured with an accuracy of 1.5% for air and 0.2 l/s for water. The maximum superficial velocities achieved in the test section are 2 m/s for water and 8 m/s for air. Optical measurements have been performed using a high-speed video camera.

Experimental campaigns have been conducted for a wide range of flow conditions

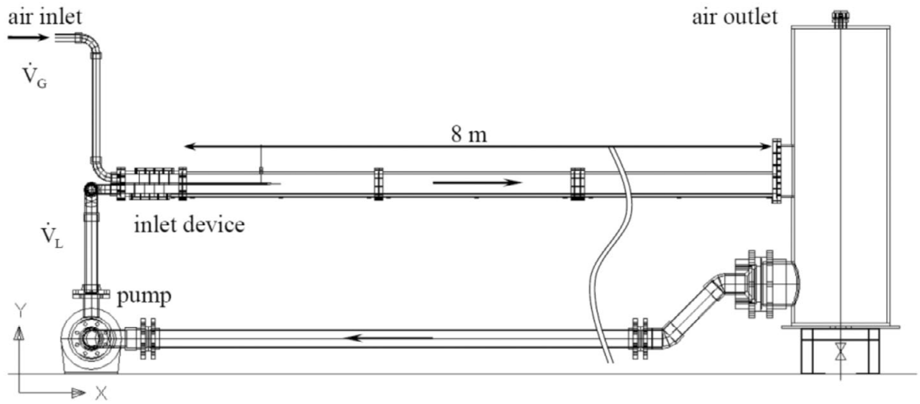

Figure 10: Scheme of the Horizontal Air/Water Channel (HAWAC) [37]

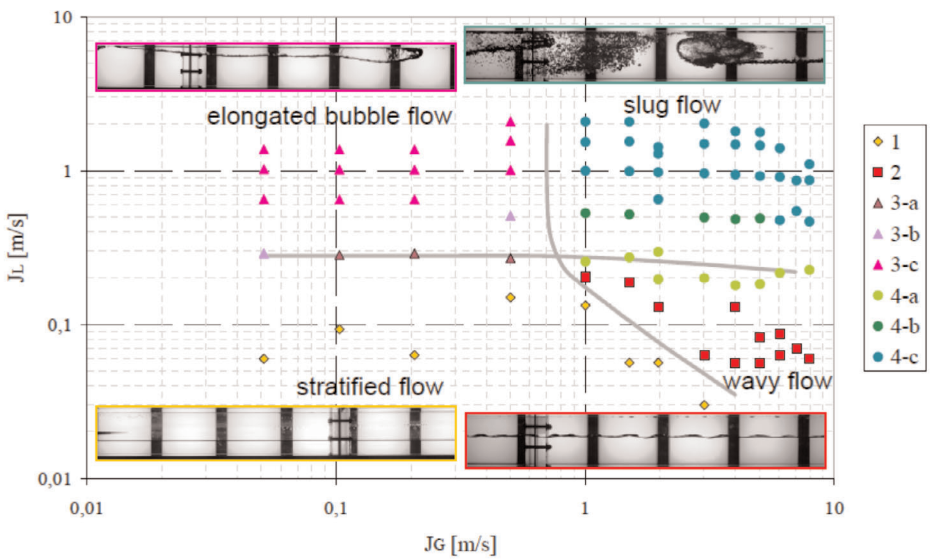

Figure 11: Tests performed and flow patter map for the channel [37]

reported in Figure 11. Several types of flows have been study: stratified, slug, wavy and elongated bubbly. Two experimental cases of slug flows have been numerically reconstructed by Vallée et al [37] with more details given for a case with 50% of air and 50 % of water.

This case is a slug flow with supercritical water and gas velocities of 1 and 5 m/s respectively. At the inlet, water was injected in the lower 50 % of the cross-section. For the computations, an initial water level of 50 mm was assumed for the entire model length. Initial temperature and pressure were 25°C and 1 atm respectively. Results show that there is a slug every 1.5 s that forms at around 2.5 m from the inlet. A sequence of photos of the quasi-periodic slug flow is shown in Figure 12. Unfortunately the starting time of the sequence is not given. Figure 12 shows the photo sequence and computed results for the slug flow. The slug moves with a measured constant velocity of 3.7 m/s. The two pressure sensors are mounted at 1.45 and 1.95 m from the inlet.

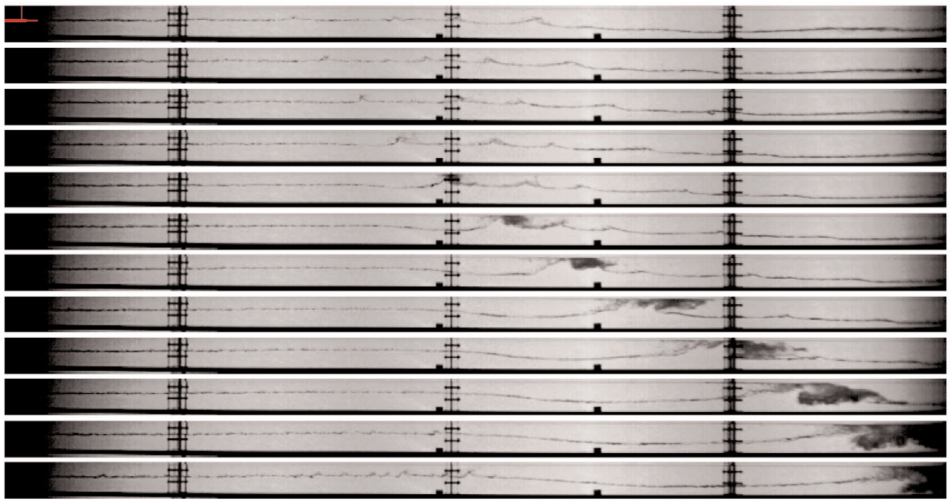

Figure 12: Picture sequence of the quasi-periodic slug flow with a Dt of 50 ms between two consecutive photos; depicted part of the channel is up to 3.2 m downstream of the inlet [37]

3.3 COMPUTATIONAL MATRIX

Using the available experimental results described in the previous sections. A computation matrix has been selected. The different cases to be computed are reported in Table 1. Most of them have been defined using the experimental work of Rahiman [5]. Among the potentialities, it has been decided to select one annular and one stratified flow. The objective is to provide a comparison between CFD calculations and the results obtained using ultrasonic tomography. The last case is the experiment carried out for slug flows by Vallée et al [37] for 50% of air and 50% of water. Since this flow has been also numerically reconstructed, this will provide the possibility to compare our numerical predictions with both experimental and computational data of Vallée et al [37].

Table 1: Computational matrix

	Type of flow	**Conditions**
Case 1 – Annular	Air (30%)-Water (70%) in a pipe	Laminar; Velocity is 3 m/s for both; No gravity
Case 2 – Stratified	Air (45%)-Water (55%) in a pipe	Laminar; Velocity is 3 m/s (for water), air is steady; with gravity
Case 4 – Slug	Air 50% — Water 50%)	Vallée [37] - Turbulent

3.4 COMPUTATIONAL CODE

To reconstruct the computational matrix of Table 1 a numerical tool has to be selected. The choice of OpenFoam [40-41] has been done since this code possesses a large number of modules for solving a wide range of flows accounting for compressibility, incompressibility, turbulence and multiphasic problems. Among the tools in open access, OpenFoam is one which has a large number of integrated models related to multiphase and turbulence problems.

The main part of the numerical activities has been the reconstruction of the experiments carried out by Rahiman [5]. The effort has been concentrated on the rebuilding of the tests performed for stratified and annular flows. The test campaigns were carried out for flows of water and air, at atmospheric pressure and room temperature of 25°C but the velocity was not specified, from the work published it is difficult to know if there were some flows or if the experiments were performed for static configuration. The pipe used for the computations had the same dimensions that the one used for the experiments:

The simulations have been carried out using a Eulerian-Eulerian approach (two-fluid model) and the VOF method. The PIMPLE [42] numerical scheme was selected for the computations. PIMPLE is a hybrid between the well-known PISO and SIMPLE solvers that allows equation under-relaxation and ensure the convergence of all equations at each time-step.

Before to proceed to the reconstruction of the computational matrix of Table 1, it has been proceeded successfully to a first code verification by computing a Poiseuille flow and turbulent flow in a circular pipe [43].

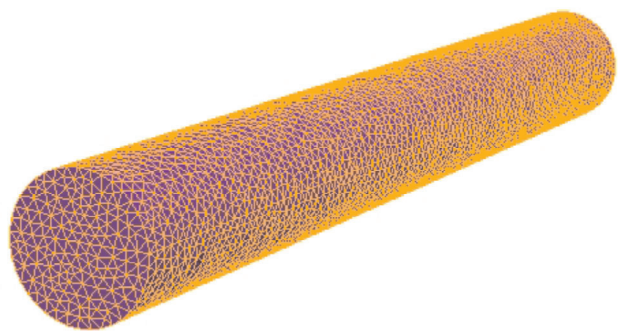

Figure 13: Mesh uses for stratified flow simulations

3.5 STRATIFIED FLOWS

The Case 1 of Table 1 is a stratified flow of air (45%) and water (55%). The pipe is in horizontal position. The pressure is 1atm, the temperature 25°C, while the inlet velocity has been set to 3m/s for both phases. This value has been taken arbitrarily. The flow is laminar and gravity is accounted for.

The unstructured mesh (see Figure 13) has been generated with Gmsh and is done of 100 000 tetrahedral elements. The pipe diameter is 103 mm, the length domain is 8 times the pipe diameter. At the exit, zero gradient conditions are applied for velocity and pressure. The numerical computations have required 50 000 iterations corresponding to 5 s of the flow in order to reach a permanent regime. The results obtained for the mass fraction are shown in Figure 14 for the cross section distribution and in Figure 15 in which the volume fraction of water is plotted along the vertical plane of the pipe. The experimental results obtained by Rahiman [5] are shown in Figure 16. The experimental data compares well with the numerical simulations since both images are nearly identical at the exception of a small region located at the left of the interface in the experiments. This small discrepancy could be due to a numerical artefact produced by the image reconstruction algorithm.

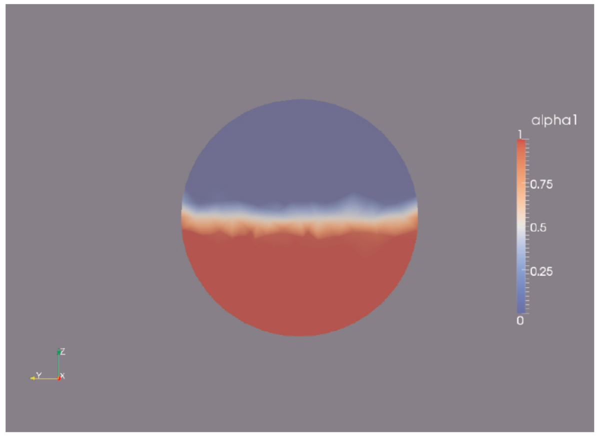

Figure 14: Volume fraction of the water in a pipe cross section (stratified flow)

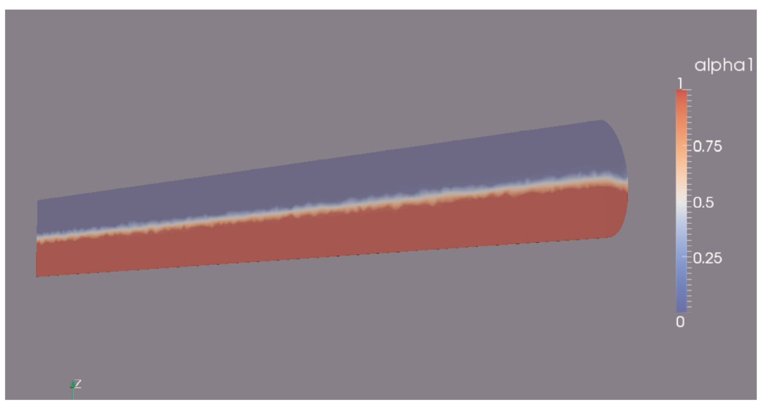

Figure 15: Volume fraction of water along the pipe (stratified flow)

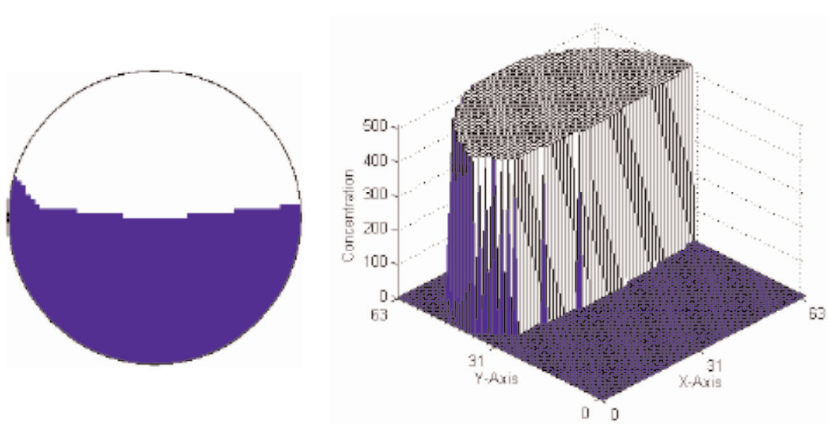

Figure 16: Fraction of water measured for a stratified flow [5]

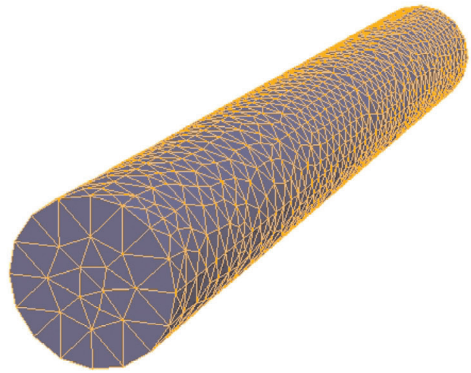

Figure 17: Mesh uses for annular flow simulations

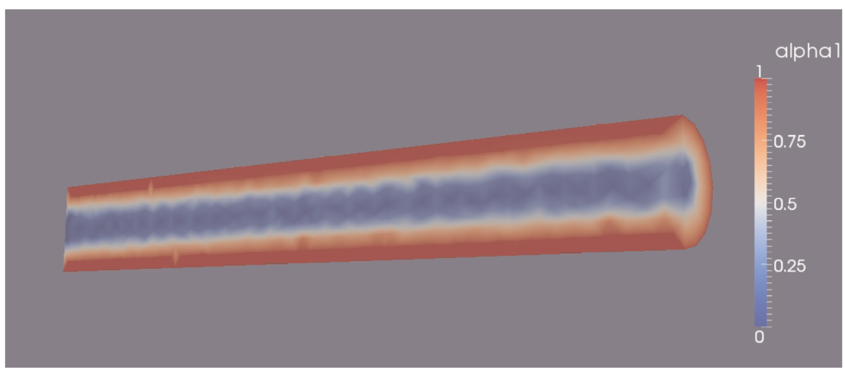

Figure 18: Volume fraction of water along the pipe (annular flow)

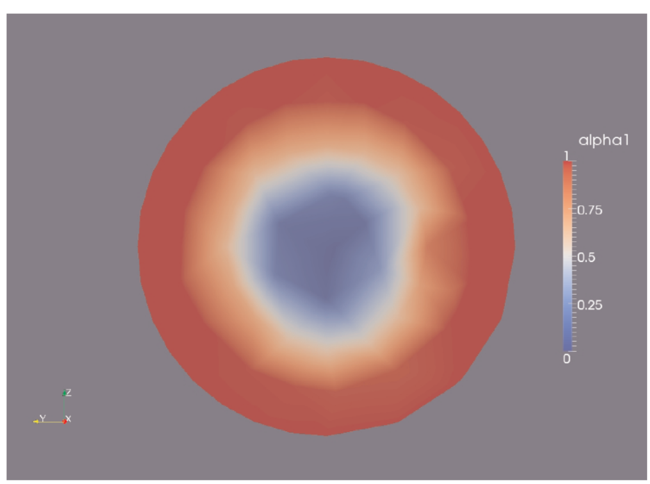

Figure 19: Volume fraction of water in the pipe cross-section (annular flow)

3.6 ANNULAR FLOWS

A similar numerical effort has been performed for the Case 2 of Table 1 that is an annular flow of air (30%) and water (70%). The pressure is 1atm, a temperature of 25°C, and the inlet velocity has been also set to 3m/s for both phases. This value has been also taken arbitrarily. The flow has been simulated for laminar conditions without accounting for gravity effects.

The unstructured mesh, shown in Figure 17, has been generated with Gmsh and it is a quite coarse mesh done of 15 000 tetrahedral elements. The pipe diameter is 103 mm, the length domain is 8 times the pipe diameter. At the exit, zero gradient conditions are applied for velocity and pressure

The numerical computations are required 50 000 iterations for simulating 5 s of the flow in order to reach the permanent regime. The volume fraction of water along the symmetry plane of the pipe is shown in Figure 18. The volume fraction of water for a cross section of the pipe is plotted in Figure 19 for the numerical predictions while the experimental results are shown in Figure 20. The comparison between both figures is fair and here the weakness

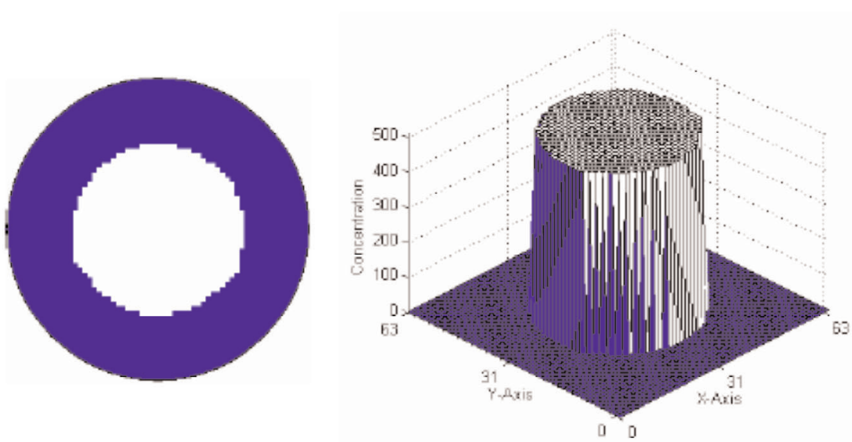

Figure 20: Fraction of water measured for an annular flow [5]

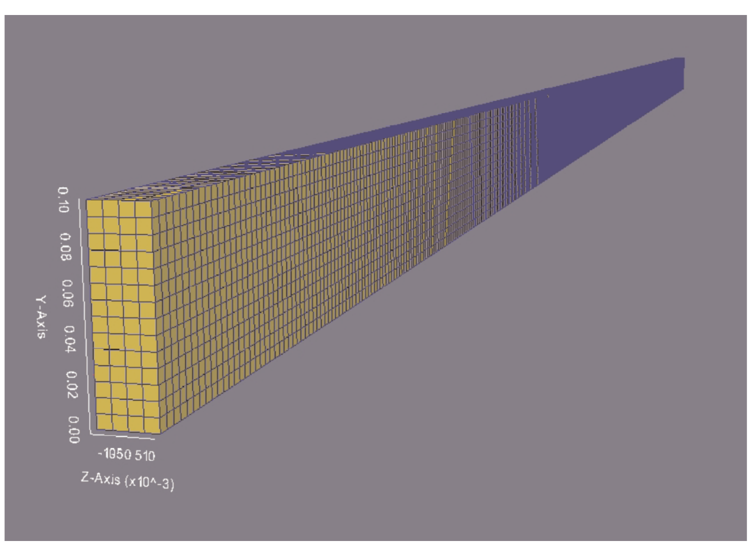

Figure 21: Mesh used for simulating the slug flow

is on the numerical simulations and is probably due to the coarse mesh. However, attempts to simulate the flow with finer grids were not successful.

3.7 SLUG FLOW RECONSTRUCTION

The final part of this activity has been the numerical reconstruction of the experiments carried out by Vallée et al [37]. This task has been undertaken to have a comparison between the numerical predictions of OpenFoam and measurements performed for a complex multiphase flow. The objective is to have a more quantitative comparison between the simulations and the experiments and also to identify potential issues when rebuilding unsteady multiphase flows. Using the experimental set-up shown in Figure 10, Vallée et al [37] have investigated slug flows for two different volume fractions of air and water with more details on the case reported in Table 1. The slug flow for these conditions (Case 3 of Table 1) has been computed and results are discussed hereafter.

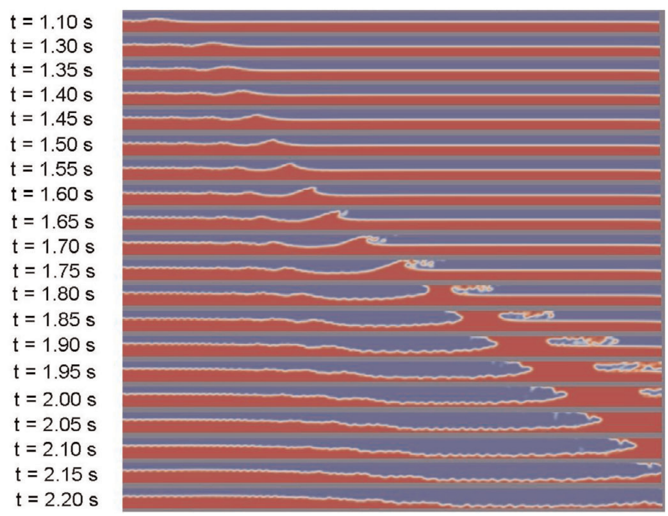

Figure 22: Unsteady distributions of the water (red) and air (blue) simulated with OpenFoam

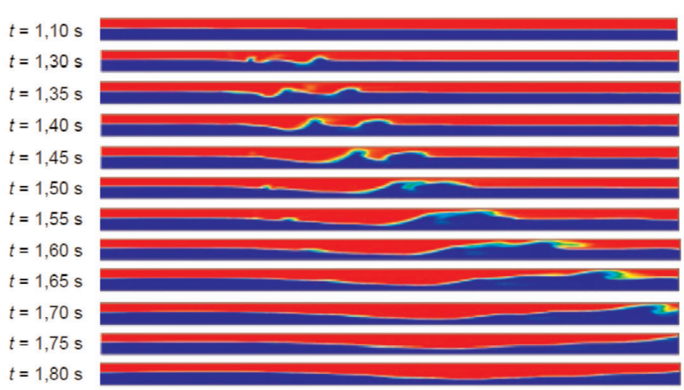

Figure 23: Numerical reconstruction carried out by Vallée et al [37] using CFX-ANSYS

Case 3 of Table 1 is a slug flow of air (50%) and water (50%). The pipe is in horizontal position. The pressure is 1atm, the temperature 25°C, while the inlet velocities have been set to 1 and 5 m/s for the liquid and gaseous phases respectively.

The mesh shown in Figure 21 has been generated with Gambit and is done of 32 000 hexahedra. The domain extents over 4 m along x, 100 mm along y and 30 mm along z which corresponds to the half of the set-up used in the tests [37]. The calculations have been carried out using the PIMPLE numerical scheme and gravity was accounted for. The flow is considered to be turbulent and the k-_ SST [44] model was retained for the calculations, the turbulence level at the inlet was selected as 5 %. At the exit zero gradient conditions are imposed for the pressure, velocity and turbulence variables.

The numerical computations have required 200 000 iterations for simulating 2 seconds of the flow in order to compare with the experiments plotted in Figure 12 and with the numerical simulations of Vallée et [37] shown in Figure 23. The unsteady results obtained for the mass fractions are shown in Figure 22. The main difference, from a modelling aspect, between the two numerical reconstructions is the VOF method used for the calculations. In the simulations of Vallée et al [37] the interface is smooth and droplets cannot be pulled out while it is possible in the current calculations.

For the two simulations and like in the experiment the slug formation starts at approximately 1.3 s. However, the comparison with the experimental data shown in Figure 12 highlights the fact that in the current simulation the slug appears at 2.5 m from the entrance while in the experiments this occurs at 1.5 m. Vallée et al [37] have observed the same discrepancy in their numerical reconstruction of their own tests. There are some differences between the experiments and the numerical reconstructions that could explain these differences. In the experiments, the velocity is increased to the nominal velocity in 0.75 s, and it is not clear of the growth is uniform (as done in the current simulation) or not. Another issue is related to the initial injection of air and water. The two fluids are injected separately in two sections separated by a blade as shown in Figure 24. The blade inclination has a strong influence on the slug length, Vallée et al [37] observed variations of 0.5 up to 3 m. Additionally, the blade produces instabilities due to the presence of its wake difficult to account when simulating the flow. A last point is the initial level of turbulence that was not measured. This is an issue since the level of turbulence at the inlet and the fact that a fully developed turbulence is present or not has a strong influence in numerical simulations.

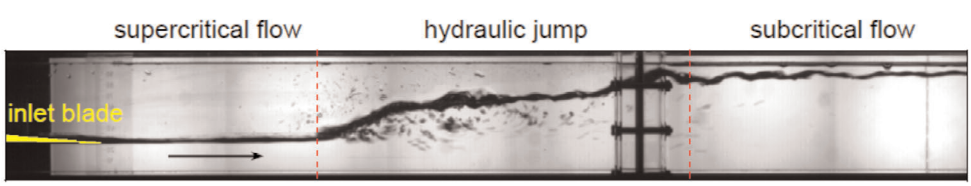

Figure 24: Hydraulic jump in the test section [37]

4. CONCLUSIONS

Tomographic techniques based on ultrasound or electrical approaches are being available for 3D mapping of multiphase flows. If progresses are still needed for improving the image reconstruction algorithms as well as the sensor capabilities, valuable results have been already produced. Both techniques can be used to perform non-intrusive measurements within metallic vessels. Among the electrical tomographic methods, multimodal tomography seems to have the best potential for future applications. The main drawback of electrical tomography techniques is their dependence on electrical properties such as conductivity and permittivity since they are temperature dependent. The recent developments of ultrasonic tomography for multiphase flow applications are very promising. This new technique is able to provide mapping of a wide range of flow conditions for large gas fractions. The main advantage of ultrasonic tomography is tis only dependence on acoustic impedance, which depends mostly on the medium density

In the frame of this activity, several experiments have been rebuilt using OpenFoam. Most of the computational effort was focused on the reconstruction of tests performed using ultrasonic tomography. The selected code has been shown capable of simulating flow in pipes this for simple and complex flow patterns. The numerical reconstruction of a slug flow has increased the confidence in the reliability of numerical simulations carried out using OpenFoam. If there is a discrepancy concerning when comparing the slug length predicted with the experimental data, it can be explained by the difficulty to reproduce the initial conditions at injection. Numerical simulations have been carried out for reproducing stratified and annular flows to compare with the results obtained by ultrasonic tomography. Comparisons between the numerical predictions and the image processed for the volume fractions highlight a good agreement between the numerical and experimental results. However, these comparisons are mostly qualitative and experimental data more detailed with numerical values for different flow variables including velocity would be an asset to fully demonstrate the capability of this technique for investigating tank sloshing.

ACKNOWLEDGMENT

The research leading to these results has been supported by the European Space Agency through ESA TAS Contract 5401000882. The authors of this paper would like also to thank Dr José Longo and Dr Lionel Marraffa from ESA/ESTEC for their valuable advices. They are also grateful to Pr. Alexandre Ouattara and Dr. Patrick Reynier from the CHU of Bordeaux for having eased the participation of one of them to the Journées d'initiation aux techniques ultrasoniques en anesthésie-réanimation.

REFERENCES

[1] Dodge, F. T., *The new dynamic behaviour of liquids in moving containers*, Southwest Research Institute, Dan Antonio, Texas, 2000.

[2] Veldman, A. E. P., Gerrits, J., Luppes, R., Helder, J. A., & Vreeburg, J. P. B., The numerical simulation of liquid sloshing on board spacecraft, *Journal of Computational Physics*, Vol. 224, pp. 82-99, 2007.

[3] Bousman, W. S., Studies of two-phase gas-liquid flow in microgravity, Ph. D. Thesis in Chemical Engineering, University of Houston, Dec. 1994.

[4] Addali, A., Monitoring gas void fraction in two-phase flow with acoustic emission, Ph D Thesis, Cranfield University, April 2010.

[5] Rahiman, M. H. F., Non-invasive imaging of liquid/gas flow using ultrasonic transmission mode tomography, Ph. D. Thesis, Universiti Teknologi Malaysia, 27 June 2005.

[6] Ahmed, W. H., & Ismail, B. I., Innovative techniques for two-phase flow measurements, *Recent patents on Electrical Engineering*, Vol. 1, pp. 1-13, 2008.

[7] Nyfors, E., Industrial microwave sensors – A review, *Subsurface Sensing Technologies and Applications*, Vol. 1(1), pp. 23-43, 2000.

[8] Ouattara, A., Principes de fonctionnement des techniques ultrasoniques, Journées d'initiation aux techniques ultrasoniques en anesthésie-réanimation, Centre Hospitalier Universitaire de Bordeaux, 16 Déc. 2011

[9] Dos Santos, S., & Prevorovsky, Z., Imaging of human tooth using ultrasound based chirp-coded nonlinear time reversal acoustics, *Ultrasonics*, Vol. 51, pp. 667-674, 2011.

[10] Holzer, K., Sadikovic, S., Esposito, L., Bockelbrink, A., Sander, D., Hemmer, B., & Poppert, H., Transcranial Doppler ultrasonography predicts cardiovascular events after TIA, *BMC Medical Imaging*, Vol. 9(13), 8p, 2009.

[11] Obajimi, M. O., Atalabi, M. O., Ogbole, G. I., Adeniji-Sofoluwe, A. T., Agunloye, A. M., Adekanmi, A. J., Osuagwu, Y. U., Olarinoye, S. A., Olusola-Bello, M. A., Ogunseyinde, A. O., Aken'Ova, Y. A., & Adewole, I. F., Abdominal ultrasonography in HIV/AIDS patients in southwestern Nigeria, *BMC Medical Imaging*, Vol. 8(5), 6p, 2008.

[12] Sconfienza, L. M., Lacelli, F., Ardemagni, A., Perrone, N., Bertolotto, M., Padolecchia, R., & Serafini, G., High-resolution, three-dimensional, and contrast-enhanced ultrasonographic findings in diseases of the eye, *Journal of Ultrasound*, Vol. 13, pp. 143-149, 2010.

[13] Holler, G., Hrach, D., & Fuchs, A., Experimental evaluation of the applicability of capacitive and optical measurement methods for the determination of liquid hydrogen volume flow, *Sensors & Transducers Journal*, Vol.6, pp. 105-116, Aug. 2009.

[14] Ohira, K., Nakamichi, K., & Kihara, Y., Develoment of a waveguide type flowmeter using a microwave method for slush hydrogen, *JSME International Journal*, Series B, Vol. 48(1), pp. 114-121, 2005

[15] Wang, F., Marashdeh, Q., Fan, L.-S., & Warsito, W., Electrical capacitance tomography: design and applications, *Sensors*, Vol. 10, pp. 1890-1917, 2010.

[16] Marashdeh, Q., Advances in electrical capacitance tomography, Ph. D. Thesis, The Ohio State University, 2006.

[17] Fan, L. S., Marashdeh, Q., & Warsito, W., 3D and real time electrical capacitance volume tomography sensor design and image reconstruction, US Patent US2010/0097374 A1, 22 April 2010.

[18] Siltanen, S., Electrical impedance tomography and Faddeev Green's function, Ph. D. Thesis, Annales Academiaescientiarum Fennicae, Helsinki, Nov. 26, 1999

[19] Polydorides,N., Image reconstruction algorithms for soft-field tomography, Ph. D. Thesis, UMIST, Manchester, Sept. 2002.

[20] Elkow, K. J., Void fraction measurement and analysis at normal gravity and microgravity conditions, Master of Science, University of Saskatchewan, Nov. 1995.

[21] Rahim, R. A., Rahiman, M. H. H. F., & San, C. K., Monitoring liquid/gas flow using ultrasonic tomography, *3rd International Symposium on Process Tomography*, Lodz, Poland, Sept. 9-10, 2004.

[22] Larsson, K., Ultrasound tomography measurements in multiphase flows, Master of Science Thesis 2000:167, Lulea Tekniska Universiteit, Sweden, 2000.

[23] Tsukamoto, A., Higashiyama, S., Yoshida, K., Watanabe, Y., Furukawa, K. S., & Ushida, T., Stable cavitation induces increased cytoplasmic calcium in L929 fibroplasts

exposed to 1-MHz pulsed ultrasound, *Ultrasonics*, Vol. 51, pp. 982-990, 2011.

[24] Delrue, S., & Van Den Abeele, K., Three-dimensional finite element simulation of closed delaminations in composite materials, *Ultrasonics*, Vol. 52, pp. 315-324, 2012.

[25] Kawashima, K., Reconstruction of the acoustic impedance profile in a plate using an inverse spectral procedure, *Ultrasonics*, Vol. 52, pp. 287-293, 2012.

[26] Mayinger, F., & Gebhard, P., Holographic measuring methods applied to two-phase flow, *Proceedings of the German-Japanese Symposium on multiphase flow*, Karlsruhe, Aug. 23-25, 1994.

[27] Mayinger, F., Two-phase flow and boiling, insights and understanding by modern non-invasive measuring techniques, *Two-Phase Flow Modelling and Experimentation*, Eds G.P. Celata & R. K. Shah, pp. 31-40, 1995.

[28] Ikeda, K., Okamoto, K., & Madarame, H., Measurement of three-dimensional density and velocity distributions using HPIV, *JMSE*, Series B, Vol. 43(2), pp. 155-161, 2000.

[29] *Multiphase Flow Handbook*, Ed. C. T. Crowe, Taylor & Francis Group, New-York, 2006

[30] Shehata, A. H., & Al Johani, M. S., A review of nuclear non-intrusive visualization methods in industry: computed tomography and particle tracking, 4th Middle East NDT Conference, Bahrain, Dec. 2007.

[31] Kumar, S. B., & Dudukovic, M., *Computer assisted gamma and X-ray tomography: Applications to multiphase flow systems*, Report DE-FC22-95PC95051, Washington University, St Louis, Missouri, Jan. 1998.

[32] Clausnitzer, V., & Hopmans, J. W., *Determination of phase-volume fractions from tomographic measurements in two-phase systems, Advances in Water Resources*, Vol. 22(6), pp. 577-584, 1999.

[33] Wu, Z., Mc Cann, H., Davis, L. E., Fontes, A., & Xie, C. G., Microwave tomographic system for oil and gas multiphase flow imaging, *Measurement Science and Technology*, Vol. 20(10), Paper 104026, Oct. 2009.

[34] Xie, C. & Wu, Z., Microwave Doppler system for multiphase flow measurement, *7th International Symposium on Measurement Techniques for Multiphase Flows*, Tianjin, Sept. 17-19, 2011.

[35] Guardiola, M., Jofre, L., Capdevila, S., Blanch, S., & Romeu, J., 3D UWB magnitude combined toographic imaging for biomedical applications. *Algorithm validation, Radioengineering*, Vol. 20(2), pp. 366-372, June 2011.

[36] Bo, O. L., Wee, A., Skjædal, I. M., Tomographic powered 3-phase flow metering in the wet gas regime, *8th International South East Asia Hydrocarbon Flow Measurement Workshop*, Kuala Lumpur, 4-6 March, 2009.

[37] Vallée, C., Höhne, T., Prasser, H.-M., & Sühnel, T., Experimental investigation and CFD simulation of slug flow in horizontal channels, Technische Berichte FZD-485, University of Dresde, Sept. 2007.

[38] Rahim, R. A., Private Communication, 24 April, 2012.

[39] Rahim, R. A., Rahiman, M. H. H. F., & San, C. K., Ultrasonic transmission-mode tomography in water/particles flow, Malaysian Science and Technology Congress, Kuala-Lumpur, 23-25 Sep. 2003.

[40] OpenFoam, *The open source CFD Toolbox, User Guide*, Version 2.1.0, OpenFoam Foundation, Dec. 11, 2011.

[41] OpenFoam, *The open source CFD Toolbox, Programmer's Guide*, Version 2.1.0, OpenFoam Foundation, Dec. 15, 2011.

[42] Ferziger, J. & Peric M., *Computational Methods for Fluid Dynamics* (2nd edition ed.), Springer, 1999.

[43] Poette, C., Evaluation de nouvelles méthodes expérimentales pour la cartographie 3D pour le ballottement des ergols, Rapport de projet de fin d'études, *Ecole Matmeca*, Institut Polytechnique de Bordeaux, 5 Sept. 2012.

[44] Menter, F. R., *Zonal two equation k-w turbulence models for aerodynamic flows*, AIAA Paper 93-2906, 1993.